

Patterning of nano-scale arrays by table-top extreme ultraviolet laser interferometric lithography

P. W. Wachulak, M.G. Capeluto¹, M. C. Marconi, C. S. Menoni, J.J. Rocca

NSF ERC for Extreme Ultraviolet Science & Technology and Department of Electrical and Computer Engineering, Colorado State University, USA

¹*Departamento de Física, Facultad de Ciencias Exactas, Universidad de Buenos Aires, Argentina*

Abstract: Arrays of nanodots were directly patterned by interferometric lithography using a bright table-top 46.9 nm laser. Multiple exposures with a Lloyd's mirror interferometer allowed to print arrays of 60 nm FWHM features. This laser-based extreme ultraviolet interferometric technique makes possible to print different nanoscale patterns using a compact table-top set up.

©2007 Optical Society of America

OCIS codes: 220.3740 Lithography, 140.7240 UV, XUV, and X-ray lasers

References and Links

1. F. J. Castano, D. Morecroft, W. Jung, and C. A. Ross, "Spin-dependent scattering in multilayered magnetic rings," *Phys. Rev. Lett.* **95**, 137201, (2005).
2. F. J. Castano, C. A. Ross, A. Eilez, W. Jung, and C. Frandsen, "Magnetic configurations in 160-520-nm-diameter ferromagnetic rings," *Phys. Rev. B* **69**, 144421, (2004).
3. F. J. Castano, C. A. Ross, C. Frandsen, A. Eilez, D. Gil, H. I. Smith, M. Redjda, and F. B. Humphrey, "Metastable states in magnetic nanorings," *Phys. Rev. B* **67**, 184425, (2003).
4. Y. Chen, A. Lebib, S. P. Li, M. Natali, D. Peyrade, and E. Cambri, "Nanoimprint fabrication of micro-rings for magnetization reversal studies," *Microelectron. Eng.* **57-8**, 405, (2001).
5. J. A. Katine, F. J. Albert, R. A. Buhrman, E. B. Myers, and D. C. Ralph, "Current-driven magnetization reversal and spin-wave excitations in Co/Cu/Co pillars," *Phys. Rev. Lett.* **84**, 3149, (2000).
6. A. Lebib, S. P. Li, M. Natali, and Y. Chen, "Size and thickness dependencies of magnetization reversal in Co dot arrays," *J. Appl. Phys.* **89**, 3892, (2001).
7. E. Saitoh, K. Harii, H. Miyajima, T. Yamaoka, and S. Okuma, "Critical phenomena in chiral symmetry breakdown of micromagnetic configurations in a nanostructured ferromagnetic ring," *Phys. Rev. B* **71**, 172406, (2005).
8. J. Aizpurua, P. Hanarp, D. S. Sutherland, M. Kall, G. W. Bryant, and F. J. G. de Abajo, "Optical properties of gold nanorings," *Phys. Rev. Lett.* **90**, 057401, (2003).
9. Y. N. Xia, J. A. Rogers, K. E. Paul, and G. M. Whitesides, "Unconventional methods for fabricating and patterning nanostructures," *Chem. Rev.* **99**, 1823, (1999).
10. M. Geissler, and Y. N. Xia, "Patterning: Principles and some new developments," *Advanced Materials* **16**, 1249, (2004).
11. W. J. Fan, S. Zhang, K. J. Malloy, and S. R. J. Brueck, "Large-area, infrared nanophotonic materials fabricated using interferometric lithography," *J. Vacuum Science Technol. B* **23**, 2700, (2005).
12. A. Fernandez, Y. J. Decker, S. M. Herman, D. W. Phillion, D. W. Sweeney, and M. D. Perry, "Methods for fabricating arrays of holes using interference lithography," *J. Vacuum Science Technol. B* **15**, 2439, (1997).
13. M. Switkes, T. M. Bloomstein, and M. Rothschild, "Patterning of sub-50 nm dense features with space-invariant 157 nm interference lithography," *Appl. Phys. Lett.* **77**, 3149, (2000).
14. H. H. Solak, "Nanolithography with coherent extreme ultraviolet light," *J. Phys. D* **39**, R171-R188, (2006).
15. H. H. Solak, C. David, J. Gobrecht, V. Golovkina, F. Cerrina, S. O. Kim, and P. F. Nealey, "Sub-50 nm period patterns with EUV interference lithography," *Microelectron. Eng.* **67-8**, 56, (2003).

16. H. H. Solak, D. He, W. Li, S. Singh-Gasson, F. Cerrina, B. H. Sohn, X. M. Yang, and P. Nealey, "Exposure of 38 nm period grating patterns with extreme ultraviolet interferometric lithography," *Appl. Phys. Lett.* **75**, 2328, (1999).
17. Y. Liu, M. Seminario, F. J. Tomasel, C. Chang, J. J. Rocca, and D. T. Attwood, "Achievement of essentially full spatial coherence in a high-average-power soft-x-ray laser," *Phys. Rev. A* **6303**, 033802, (2001).
18. Y. W. Liu, M. Seminario, F. J. Tomasel, C. Chang, J. J. Rocca, and D. T. Attwood, "Spatial coherence measurement of a high average power table-top soft X-ray laser," *Journal De Physique IV* **11**, 123, (2001).
19. I. Junarsa, M. P. Stoykovich, P. F. Nealey, Y. S. Ma, and F. Cerrina, "Hydrogen silsesquioxane as a high resolution negative-tone resist for extreme ultraviolet lithography," *J. Vacuum Science Technol. B* **23**, 138, (2005).

1. Introduction

Regular arrays of metallic or semiconductor nano pillars and nanorings with sizes sub 100 nm have lately attracted great attention due to their unique optical, electrical and magnetic properties¹⁻⁸. Different strategies have been used for the fabrication of these arrays, including photo and electro beam lithography, self assembly of nanospheres or replication by embossing, molding or printing with masters stamps⁹. In the case of self assembly the arrangement of nanostructures is often random, or organized in reduced areas. The replication using master stamps have demonstrated features sizes below 100 nm and large area coverage¹⁰. However, a different master is necessary for each motive restricting the versatility of the method.

An approach commonly used to print nano-scale periodic features is interferometric lithography (IL). This maskless photo-lithographic technique is based on the activation of a photoresist by the interference pattern generated by two or more spatially coherent light beams. IL can efficiently print periodic patterns in a sensitive photoresist coated substrate with resolution approaching half of the wavelength of the illumination. In this approach, reducing the wavelength of the illumination provides a direct and simple path to realizing interference patterns with dimensions of tens of nanometer and below. This has been the main motivation for using ultraviolet¹¹⁻¹³ and even shorter wavelength extreme ultraviolet (EUV) light for this application¹⁴⁻¹⁶. The versatility of EUV IL for patterning different motifs and realizing record small features has been demonstrated using 13 nm wavelength light from a synchrotron source¹⁶. However, the widespread use of this technique in applications requires its implementation on a more compact and easily accessible set-up.

2. Experimental details

In this paper, we report the demonstration of multiple exposure IL using a table-top set up based on a compact $\lambda = 46.9$ nm capillary discharge laser. This simple and compact set up enabled printing of arrays of cone-shaped nano-dots with 60 nm FWHM diameter with a periodicity of 150 nm using exposure times of less than 1 minute. As discussed below, the high degree of spatial and temporal coherence of capillary discharge EUV lasers makes them well suited for IL experiments. These results highlight the potential of table-top EUV lasers for the realization of a compact wide-area nanopatterning system.

The illumination source used in this work is a compact $\lambda = 46.9$ nm Ne-like Ar capillary discharge laser configured to produce pulses with energy of approximately 0.2 mJ and about 1.2 ns FWHM duration. When operated at repetition rates of several Hz this table-top laser can produce EUV beams with average powers in excess of 1 mW and a high degree of spatial and temporal coherence¹⁷. The 27 cm long capillary discharge plasma columns used in this experiment generates a laser beam that has a spatial coherence length of approximately 570 μm measured at the experiment chamber located at 1.7 m from the exit of the laser. The spatial coherence length can be further increased using a longer plasma^{17,18}. The laser beam temporal coherence is greater than 470 μm as determined by its line width $\Delta\lambda/\lambda < 1 \times 10^{-4}$.

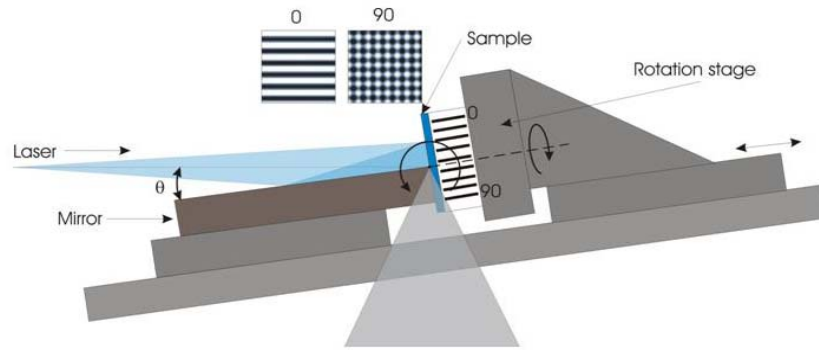


Fig. 1. Lloyd's mirror set up for two steps exposure. The sample is rotated an arbitrary angle around an axis perpendicular to the sample surface to obtain different motifs.

IL was implemented by illuminating a flat mirror in the Lloyd's configuration with the EUV laser output. In this configuration, part of the laser beam impinges on the mirror at an incidence angle θ and is reflected to interfere with the remaining un-deflected portion of the beam, as illustrated in Fig. 1. Beam interference gives rise to a sinusoidal intensity pattern of period d , defined by the wavelength of the light λ and the incidence angle θ according to $d = \lambda / (2 \sin \theta)$. Figure 1 shows a schematic of the set up utilized in the experiment. A rectangular $30 \times 50 \text{ mm}^2$ Cr coated flat mirror was mounted at grazing incidence in front of the laser beam on a pivoting platform, with its axis coincident with the farther edge of the mirror. The sample, consisting of a Si wafer coated with poly-methyl methacrylate (PMMA), was mounted at this edge of the mirror in a motorized rotation stage. Controlled rotation by an angle α around an axis normal to the sample's surface allows for multiple exposures. A translation stage retracts the sample from the mirror edge before each rotation. The entire system was mounted on a motorized pivoting platform that allows changing the incidence angle θ . The Lloyd mirror interferometer system was housed in a vacuum chamber $0.45 \times 0.55 \times 0.40 \text{ m}^3$ that was differentially pumped respect to the laser to maintain a pressure of approximately 10^{-5} Torr. The entire EUV interferometry instrument has a footprint of $0.7 \times 2.6 \text{ m}^2$.

3. Results

To pattern an array, a PMMA coated sample was initially exposed to produce an interference pattern consisting on regular lines parallel to the mirror's edge. This was followed by a second exposure in which the sample was rotated in situ by an angle $\alpha = \pi/2$. This procedure was carried out without necessity to break vacuum thus assuring similar conditions for both exposures. Typical exposure times of 30-50 seconds were used to print periodic patterns over surface areas of $500 \times 500 \mu\text{m}^2$. Ultra thin photoresist layers, approximately 30 nm thick, were deposited on the sample to match the thickness of the photoresist layer to the penetration depth of the 46.9 nm in PMMA, allowing the photolithographic pattern to reach the substrate. This was accomplished by spin coating the substrate with diluted 1% PMMA in Anisole at 5000 RPM in a standard spin coater. After the exposure the PMMA was developed with the standard procedure consisting of an immersion in a 1:3 solution of MIBK-methyl isobutyl ketone (4-Methyl-2-Pentanone) with IPA-isopropyl alcohol for 35 seconds, followed by rinsing with IPA. The sample was subsequently dried using compressed nitrogen.

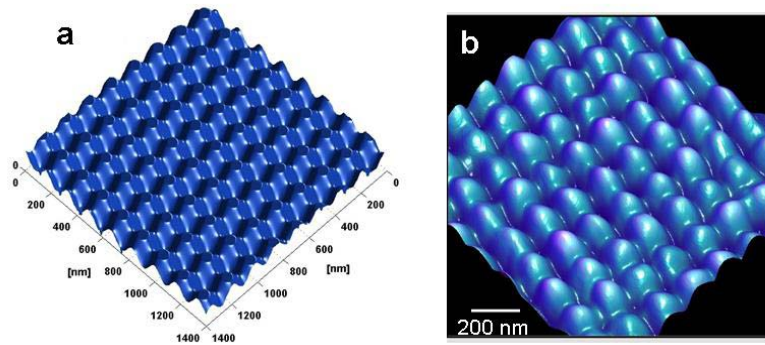


Fig. 2. Computed (a) and fabricated (b) arrays of holes patterned in PMMA by double exposure with a Lloyd's mirror configuration, $\alpha = \pi/2$ and low (10 mJ cm^{-2}) photon dose.

The photon dose applied in each exposure, calculated as the energy per unit area, allows an extra degree of control over the shape of the features imprinted. The thickness of photoresist left in the exposed areas after the development process (residual thickness) is a linear function of the applied dose. For PMMA the residual thickness was measured by Junarsa et al.¹⁹. Using these data we calculated the patterned profile obtained for a double exposure as a function of the applied dose. Figure 2a shows the calculated profile obtained in a PMMA layer for a low dose exposure of 10 mJ cm^{-2} . The pattern was calculated by superposing of two identical interference patterns rotated by an angle $\alpha = \pi/2$. For a dose of 10 mJ cm^{-2} , which can be obtained with about 20 laser shots, the simulation shows that the photoresist is only activated along lines coincident with the interference maxima, leaving in the crossing points small regions where small holes are developed. A similar pattern is obtained experimentally, as shown in figure 2b where a small $1.4 \times 1.4 \mu\text{m}^2$ section of the total printed surface was scanned with an atomic force microscope (AFM) used in tapping mode with a 10 nm tip size cantilever.

If the applied dose is increased to 32 mJ cm^{-2} (high dose), the loci in the sample surface with sufficient exposure to activate the photoresist are broader. In this case the activated volume generates after development a regular array of trenches in two perpendicular directions that leave small non activated spots at the intersections. Figure 3a is the calculated pattern corresponding to the high dose exposure. The experimental pattern is shown in figure

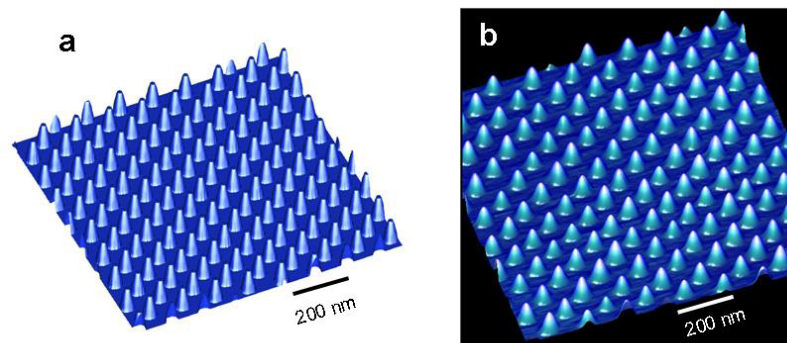


Fig. 3. Computed (a) and fabricated (b) arrays of cone-shaped nano-dots patterned in PMMA by double exposure with a Lloyd's mirror configuration, with $\alpha = \pi/2$ and high (30 mJ cm^{-2}) photon dose.

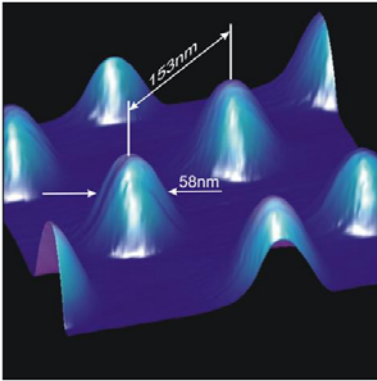


Fig. 4. Magnified view of a smaller area of the array in figure 3, showing the cone-shaped nano-dots. The FWHM of the nano-dot is approximately 60 nm and the period is nominally 150 nm.

3b and corresponds to a very regular array of cone-shaped dots that closely resembles the simulation. The period, 150 nm in this example, can be continuously changed by varying the incidence angle θ . The FWHM of the features is approximately 60 nm. Figure 4 shows a detail of the measured profile where the period and the FWHM of the cone-shaped dots are indicated. The height of the cones corresponds to the penetration depth of the 46.9 nm light in the PMMA, approximately 30 nm.

4. Summary

In summary, we have realized nanometer-scale patterning using a table-top system by interferometric lithography. Using a multiple exposure Lloyd's mirror configuration dense arrays of holes and nanodots with feature size as small as 60 nm were imprinted in PMMA over areas in excess of $500 \times 500 \mu\text{m}^2$ using a 46.9 nm wavelength laser. The periodicity of the structures can be controlled by changing the incidence angle of light beam at the mirror while the minimum size of the feature can be varied by changing the applied dose.

These results show that table-top EUV lasers combined with interferometric lithography schemes are a useful compact alternative for printing nanometer size features. The table top EUV-IL approach, used in concert with compact table top lasers, brings into the laboratory environment all of the advantages of this technique which implementation was previously restricted to large synchrotron facilities.

Acknowledgements

This work was supported under the NER program, NSF Award DMI-0508484 utilizing facilities from the NSF ERC for Extreme Ultraviolet Science and Technology, Award Number EEC-0310717. MGC acknowledges the support through a fellowship from CONICET.